

Site-specific Eu(III) binding affinities to a *Datura innoxia* biosorbent

Debbie D. Serna, Jessica L. Moore, Gary D. Rayson*

Department of Chemistry and Biochemistry, New Mexico State University, Box 30001, MSC 3C, Las Cruces, NM 88003, United States

ARTICLE INFO

Article history:

Received 28 April 2009

Received in revised form 21 August 2009

Accepted 21 August 2009

Available online 27 August 2009

Keywords:

Datura innoxia

Metal ion binding

Biosorption

Binding affinities

ABSTRACT

The binding of Eu(III) to a biosorbent derived from cultured cells of the plant *Datura innoxia*, have been investigated through elucidation of apparent affinity constants associated with different chemical environments present on the cell wall. Adsorption isotherms for separate types of binding sites were generated using metal ion luminescence measurements. Application of regularized regression analysis to these isotherm data for four chemically distinguishable sites revealed the presence of sites exhibiting both low (mean $\log K_{app} = -0.3$ to 0.6) and higher (mean $\log K_{app} = 3.2$ –3.5) apparent affinities for pH conditions of 2.0, 4.0, and 5.0. Low affinity sites were observed for all pH conditions and attributed to non-specific binding of the metal ions to the negatively charged biomaterial. The pH-dependent higher affinity sites are ascribed to specific sites involving either an ion-exchange mechanism or formation of weak surface–metal ion complexes. These results differed significantly from a similar analysis of total metal binding isotherms that indicated mean $\log K_{app}$ values of -0.5 to 0.25 (low affinity) and 5.6–6.0 (high affinity).

© 2009 Elsevier B.V. All rights reserved.

1. Introduction

Use of biological materials for the removal of heavy metals from contaminated water provides many advantages relative to synthetic sorbents [1,2]. Many of the characteristics of these materials can be ascribed to the diversity of chemical binding sites found on such biosorbents [3]. However, this chemical heterogeneity provides the greatest barrier to the implementation of these materials in treatment and remediation systems [4]. An incomplete understanding of the chemical characteristics of these varied metal binding sites limits the predictability of metal ion biosorption dependence on solution pH and salinity [1,5].

Chemical heterogeneity of binding sites is an inherent characteristic of biomaterials that can result from either the existence of multiple binding functionalities or the presence of specific functionalities in various molecular environments. Amino, sulfhydryl, carboxyl, carbonyl, phosphate, sulfate, phenolic, and amide moieties have all been suggested as possible functionalities involved in metal ion binding [6,7]. However, recent work has indicated the predominate involvement of oxo-type moieties including carboxylates, sulfonates, and phosphates [1].

Spectroscopic tools have been used to identify the responsible chemical functional groups. These have included nuclear magnetic resonance (NMR) [8,9], X-rays absorption techniques (e.g., near edge absorption and extended absorption fine structure) [10,11],

and metal luminescence [4]. Unfortunately, these techniques have been limited to spatial averaging of the varied metal ion binding chemistries involved with these heterogeneous materials. Eu(III) luminescence enabled to identification of four chemically distinguishable binding environments on a biomaterial derived from the plant *Datura innoxia* [4]. Unfortunately, quantitative contribution of each environment was not possible using their experimental configuration.

Other work has been directed toward understanding the interactions of metal binding to each biomaterial [12]. Such studies involved the analysis [13] or modeling [14,15] of adsorption isotherms derived from the total amounts of metal ion bound to the material with varied solution conditions (i.e., initial metal concentration and solution pH).

Borkovec and co-workers [16] have described the use of regularized least-square methods to obtain affinity distribution functions for the interaction between metal ions and heterogeneous sorbents. Regularized least-square methods were employed to resolve problems (such as instability) associated with many proposed approaches.

The program (QUASI) developed by those researchers is based on this algorithm and previously was used for the extraction of affinity distribution of Pb^{2+} ions to immobilized *D. innoxia* cultured cell fragments [17]. Effects of solution conditions such as ionic strength and pH on the resulting affinity distributions were studied. Involvement of both high apparent affinity (mean $\log K_{app} \sim 5.3$) and low apparent affinity sites (mean $\log K_{app} \sim 2.5$). These were reported to result from either surface complexes or ion-exchange processes, respectively. Unfortunately, that study was limited to

* Corresponding author. Tel.: +1 575 646 5839; fax: +1 575 646 2649.
E-mail address: garayson@nmsu.edu (G.D. Rayson).

investigation of the total amount of metal ion bound. The present study extends the application of this approach to enable spectroscopic resolution of Eu(III) binding environments.

Specifically, the mechanisms of metal ion sorption to a biosorbent derived from cultured anther cells from *D. innoxia* have been investigated [4]. Eu(III) luminescence spectroscopy has enabled the identification of four chemically different binding sites involving carboxylate and sulfate functionalities with on class of sites involving the polysaccharide structure of the cell wall [18]. However, the inability of the laser excitation source used in those earlier studies to optically saturate the 5D_0 excited state of the Eu(III) enabled only qualitative interpretation of the data.

Attainment of optical saturation of the Eu- 5D_0 excited state within the present study enables quantification of metal binding to each site-type. Determination of the amount of metal bound under varied solution pH enabled, for the first time, generation of pH-dependent affinity spectra for each Eu(III) metal ion binding site on the *D. innoxia* biomaterial.

2. Experimental

2.1. Sample preparation

The *D. innoxia* biosorbent used in these studies consisted of lysed cells from the anther (flower) of the plant. These cultured cells were selected to minimize tissue variability. Growth conditions have been described elsewhere [18]. Briefly, this involved development in a Gamborg's 1B5 medium supplemented with vitamins [19]. Following harvesting, the cells were lysed in an ethanol solution and dried. Native metals associated with the material were removed by washing in a 1.0 M HCl solution [20]. Dried cell wall fragments were then ground and the <200 mesh size fraction (<127 μm) collected for future study.

Metal solutions were prepared by serial dilution of either a 1000 ppm or 1.0 M stock solution. The stock solutions were prepared by dissolution of Eu_2O_3 (Aldrich, 99.99%) in dilute HNO_3 (1.0 M). Subsequent metal ion solutions were prepared in solutions of the sodium form of a 0.1 M 2-(*N*-morpholino) ethanesulfonic acid (MES). This salt was included to control the ionic strength of each solution without introducing a potential complexing ligand [21]. Solution pH was adjusted through drop-wise addition of either concentrated HCl or a saturated solution of NaOH using a pH combination electrode (Orion, model 710A).

Individual samples were prepared by weighing out triplicate 30 mg samples of the biomaterial into separate 3.5 mL polypropylene test tubes for each condition of solution pH (2.0, 4.0, or 5.0) and metal ion concentrations (5, 10, 20, 50, and 100 ppm and 5.0, 10.0, 20.0, 50.0 and 100.0 mM). A total of 3.0 mL of each respective solution was added to each sample and an equal volume added to an empty test tube as a control. The pH of each solution was then measured and recorded.

Both samples and controls were placed on a rocker for 1 h and centrifuged (Sorvall, GLC-2B) at 3000 rpm for 30 min. Resulting supernatant solutions were decanted for analysis. Remaining biomaterial pellets were freeze-dried. A 10.0 mg portion of each sample was encapsulated within a glass matrix consisting of 150 mg KBr.

The amount of europium bound to each biomaterial sample was calculated using Eq. (2)

$$q_{\text{Eu}} = \frac{(C_c V_c - C_s V_s)}{m_s} \quad (1)$$

where C_c and C_s are the measured equilibrium europium molar concentrations in the control and sample solutions, respectively. Supernatant and control solutions were analyzed by inductively coupled plasma atomic emission (ICP-AES, PerkinElmer, model

Optima 4300DV-Dual View, Norwalk, CT). The variables V_c and V_s represent the volumes for the respective solutions and m_s is the mass of biomaterial.

2.2. Luminescence measurements

The local chemical environments of the bound Eu(III) were probed using laser-excited luminescence [18]. Fig. 1 depicts a schematic of the instrumentation used. This configuration has been described previously [18] with significant differences. This involved use of a relatively high fluence Nd:YAG-pumped dye laser system (Quanta-Ray, models DCR and PDL-1, respectively) rather than a N_2 laser-pumped dye laser assembly as the scanned excitation source [18]. This laser system enabled the optical saturation of the 5D_0 excited-state of the bound Eu(III). Relaxation of the excited metal ions to the 7F_2 state was monitored at 615.00 nm. Using an optical configuration described elsewhere [22], the emitted radiation was isolated using a 1.0 m focal length monochromator (McPherson Instruments, model 2051) and detected with a photomultiplier tube (PMT_{sig} , Hamamatsu Corp., model R955).

The average radiant energy of the ~ 10 ns dye laser pulses was measured to be $450 \mu\text{J pulse}^{-1}$ using an energy meter (model Rj-7100, Laser Precision Corp., Utica, NY). A condition of optical saturation of the excited state was confirmed by recording the measured luminescence intensity while systematically attenuating the incident beam intensity by the use of neutral density filters of increasing optical density. Optical saturation of the 5D_0 state of the Eu(III) bound to the biomaterial was experimentally verified.

Native luminescence arising from molecular species within the *D. innoxia* material was addressed by the incorporation of time-gating PMT electronics (model C1392-56, Hamamatsu Corp.) and using a 15 μs delay (Digital Delay Generator, model 7010, Berkeley Nucleonics Corp., Berkeley, CA) relative to the incident laser pulse detected by PMT_{ref} (Fig. 1). This enabled the decay of the

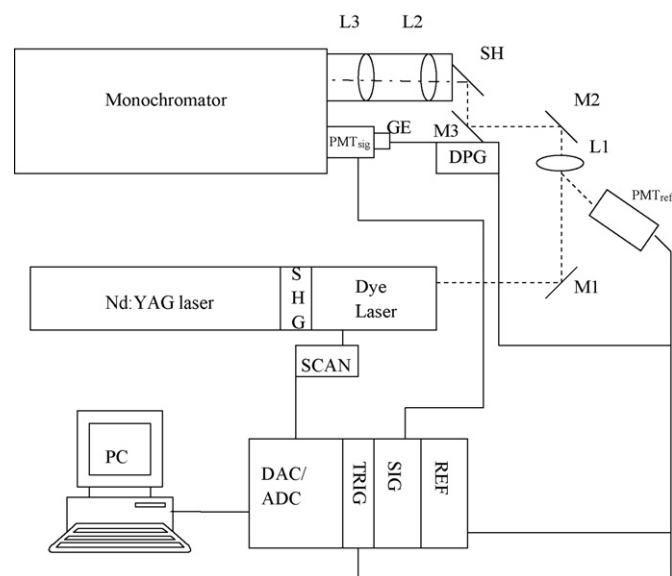


Fig. 1. Schematic representation of experimental configuration. Output from an Nd:YAG laser undergoes second harmonic generation (SHG) to pump a dye laser. This is directed onto the sample using a series of turning mirrors (M1, M2, and M3) and is focused using lens L1. Emitted radiation is collimated by lens L2 and focused on the entrance slit of the monochromator using L3. Light is detected using a photomultiplier tube, PMT_{sig} , that is gated with the output of a delayed pulse generator (DPG) that is triggered by the signal from the reference PMT (PMT_{ref}). Reference and signal magnitudes are further processed using boxcar gated integrators (REF and SIG). Both data acquisition and scanning of the excitation wavelength are controlled by a personal computer (PC), using a scan controlling stepper motor, SCAN.

short-lived native luminescence prior to the detection of the Eu(III) luminescence ($\tau \geq 100 \mu\text{s}$) [18].

2.3. Data analysis

Luminescence excitation spectra. Because of the non-degeneracy of both the ground (7F_0) and excited (5D_0) states of Eu(III), variation in the local chemical environment of the metal binding sites results in shifts of single Lorentzian spectral lines [19]. The presence of multiple binding environments then produces multiple features within the measured excitation spectral envelop [18]. Mathematical deconvolution of features has been shown to enable the identification of those chemical environments upon comparison with spectra of model metal–ligand systems [18]. Under conditions of optical saturation of the 5D_0 state, it was possible to relate the respective areas of these deconvoluted peaks to the amount of metal ion bound to each site based on mass balance calculations of the total metal bound under each condition.

Deconvolution of the measured 5D_0 excitation spectra was achieved through the application of a Levenberg–Marquardt algorithm with GRAMS-3D (Galactic Industries Corp., Salem, NH). Earlier investigations of Eu(III) binding to this biomaterial reported the involvement of as many as four distinct binding environments [18]. Deconvolution of the present spectra was thus limited to these same spectral components. Curve-fitting parameters included: (1) the location of each peak maximum, (2) the magnitude of each peak, and (3) the relative amounts of Gaussian and Lorentzian character given to the shape of each peak (theoretically, each peak should exhibit a Lorentzian line shape [19]). Every effort was made to eliminate operator bias during data analysis.

As mentioned above, affinity distributions were determined from the Eu(III) ion binding isotherms using the program QUASI. This program has been described elsewhere [16]. The program QUASI includes assumptions of 1:1, metal ion:ligand site, complex formation, the presence of stoichiometric ratios, Langmuirian binding behavior for each site, and a linear superposition of local isotherms comprising the total sorption isotherm. A major constraint within the program disallowed negative site concentrations. Three regularizing functions were used including smoothness, a small number of sites, and maximum entropy. A smoothness regularizing function enabled calculation of continuous affinity distributions. The constraint of a small number of sites was also employed to generate the minimum number of sites required to adequately describe the system. Application of regularized methods minimizes instabilities in the resulting distributions.

Typical parameters of QUASI used in this study included a “spectral” window of $\log K_{\text{app}} = -2.0$ to 5.0, a grid spacing of 0.03, and the regularization parameter 1. The non-negative site constraint and the smoothness regularizing function were employed. No constant or linear isotherm was applied [16].

3. Results and discussion

Fig. 2A shows the binding isotherms for total metal binding to the *D. innoxia* material under solution conditions of pH 2.0, 4.0, and 5.0. Readily visible are several regions of metal binding. At high metal ion concentrations, the amount of metal bound varied linearly with the remaining equilibrium solution concentration. This behavior is consistent with non-specific electrostatic attraction of the positive metal cations to a negatively charged material under conditions of high metal ion concentration (i.e., 20–80 mM). This interpretation can be supported by considering the following reaction to describe such an interaction:



where Ch^{n-} represents the presence of non-specific charges near the surface of the biosorbent and $\text{MCh}^{(n-3)-}$ the metal ion associated with the biomaterial by electrostatic attraction. This can be described by the equation:

$$K_{\text{es}} = \frac{[\text{MCh}^{(n-3)-}]}{[\text{M}^{3+}][\text{Ch}^{n-}]} = \frac{q_{\text{M}}}{[\text{M}^{3+}]_{\text{eq}}[\text{Ch}^{n-}]} \quad (3)$$

where the amount of bound metal ion, q_{M} , is defined as the moles of metal ion bound per gram of biomaterial. If the number density of non-specific charges is a function of the material and therefore constant for a given biomaterial, Eq. (4) can be rewritten as:

$$q_{\text{M}} = [\text{M}^{3+}]_{\text{eq}}(K_{\text{es}}[\text{Ch}^{n-}]) \quad (4)$$

This would then be predicted to yield a linear relationship between the measured quantities of q_{M} and $[\text{M}^{3+}]_{\text{eq}}$, such as is shown in Fig. 2A.

Observed increased binding by this mechanism at pH 2 may result from a removal of surface charged functionalities by increased protonation of weak acid moieties (e.g., carboxylates). Two additional regions were also observed for lower concentrations exhibiting the more conventional, non-linear behavior (Fig. 2A). These isotherms suggest the presence of high affinity sites that appear to experience saturation with increased metal ion concentration.

The affinity spectra shown in Fig. 2B correspond to the application of the regularized regression analysis of the isotherms shown in Fig. 2A, as described above. Two classes of binding environments were revealed. Similar to those described by Lin, et al. for Pb^{2+} binding [17], the collection of high affinity sites could be attributed to the formation of a surface–metal complex while the low affinity

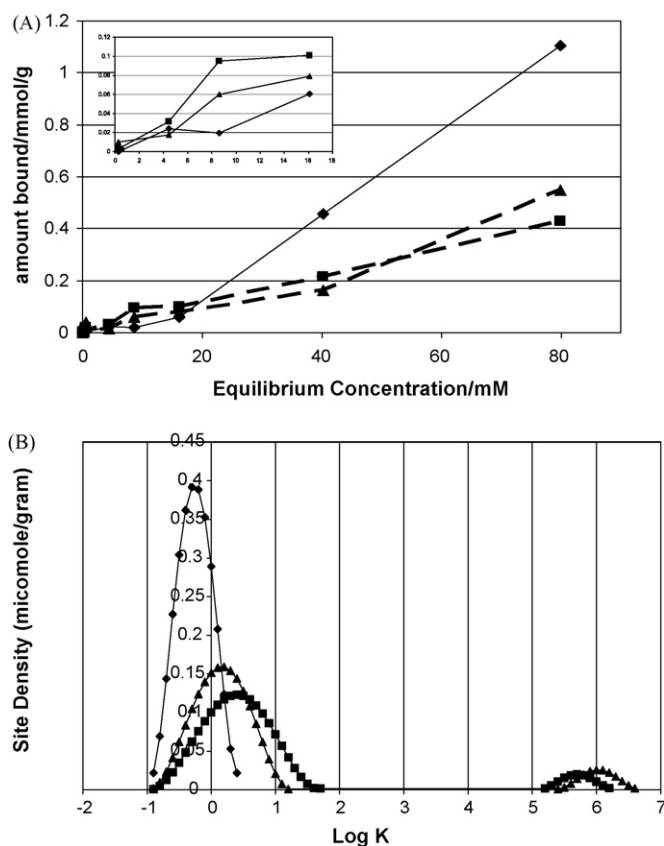


Fig. 2. (A) Binding isotherms for europium ions to *Datura innoxia* biosorbent and (B) the corresponding affinity spectra at solution pH values of 2.0 (◆), 4.0 (▲), and 5.0 (■).

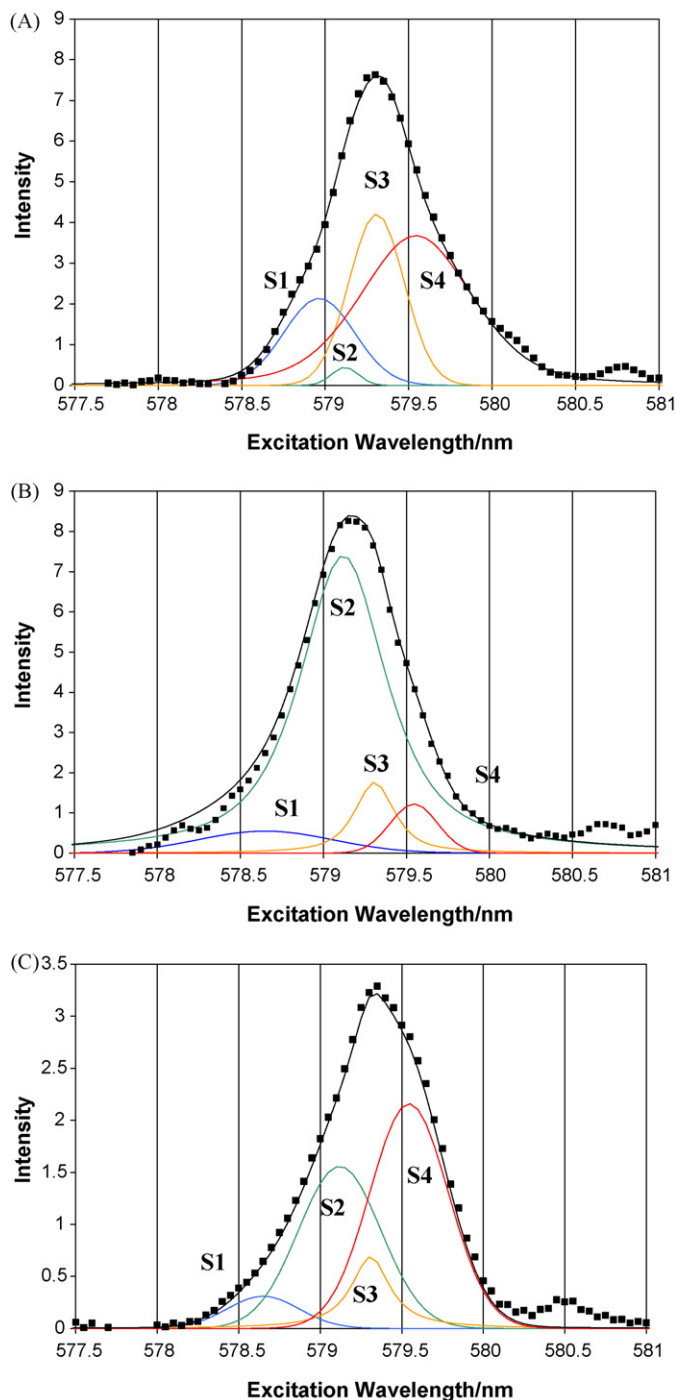


Fig. 3. Excitation spectra for Eu(III) bound to *Datura innoxia* when exposed to a 50 mM solution of Eu(III) (■) under pH conditions of (A) 2.0, (B) 4.0, and (C) 5.0. Deconvoluted peaks assigned to binding to sites 1 through 4 with their sum.

sites to metal ion binding by an ion-exchange process. However, Lin et al. [17] observed the apparent affinity constant for their ion-exchange sites to remain relatively constant with solution pH. These results indicate a measurable dependence of the calculated apparent affinity constants on solution pH. A pH-dependence of the K_{app} was earlier attributed to metal complex formation, a conclusion that appeared to be inconsistent with lower apparent affinities. Additionally, the magnitudes of apparent affinities for these sites are significantly lower than those reported by Lin et al. for lead ion-exchange binding sites [17]. Clearly additional investigation of Eu(III) binding to this material was required.

Representative average excitation spectra for Eu(II) bound to the *D. innoxia* biosorbent for an initial metal ion concentration of 50 mM at each solution pH (2.0, 4.0, and 5.0) are shown in Fig. 3. Also shown are the four individual peaks resulting from the deconvolution of each spectral envelope. Although the locations of the individual spectral components were not defined prior to peak deconvolution, the resulting features exhibited marked similarities (Fig. 3). This provided increased confidence in the assignment of each component to separate metal ion binding sites present on the *D. innoxia* cell walls.

Review of the results illustrated in Fig. 3 reveals several trends. For all conditions, the peak for site 1 was observed as a broad, more Gaussian peak of lower relative intensity. This could be indicative of an ensemble of chemically similar sites resulting in an increase

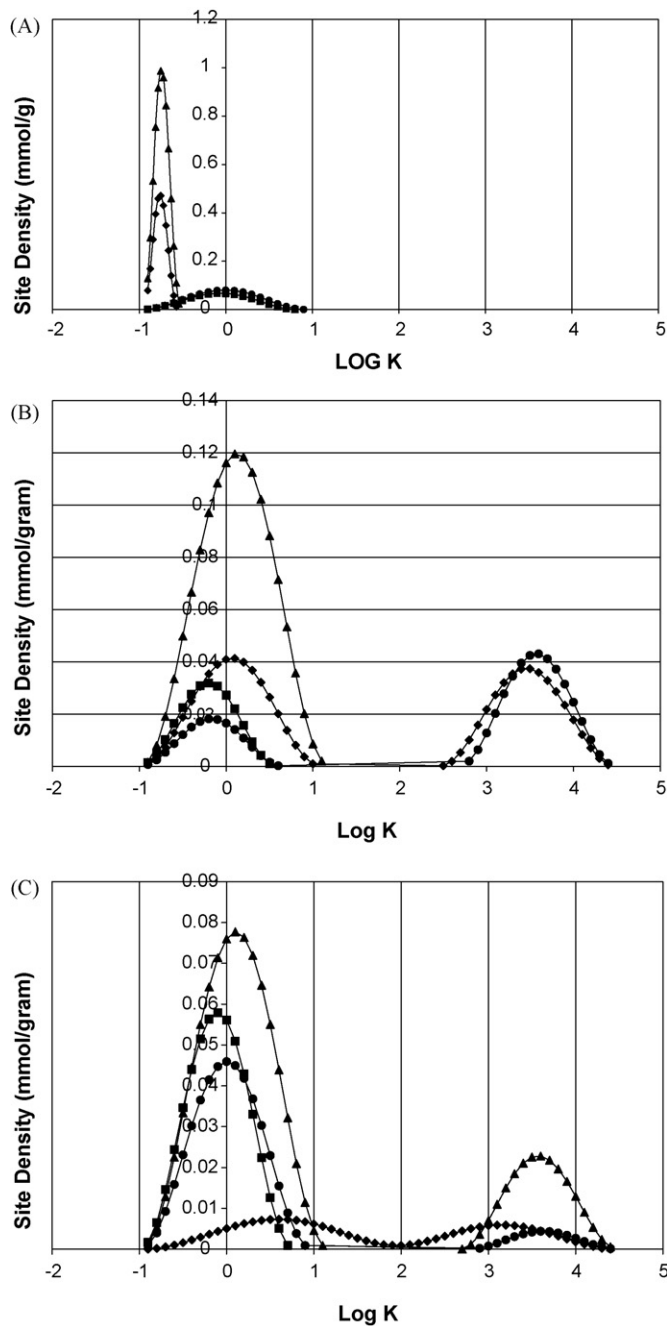


Fig. 4. Affinity spectra derived from binding isotherms generated from deconvoluted excitation peak areas for site 1 (◆), site 2 (▲), site 3 (■), and site 4 (●) under solution conditions of pH 2 (A), pH 4 (B), and pH 5 (C).

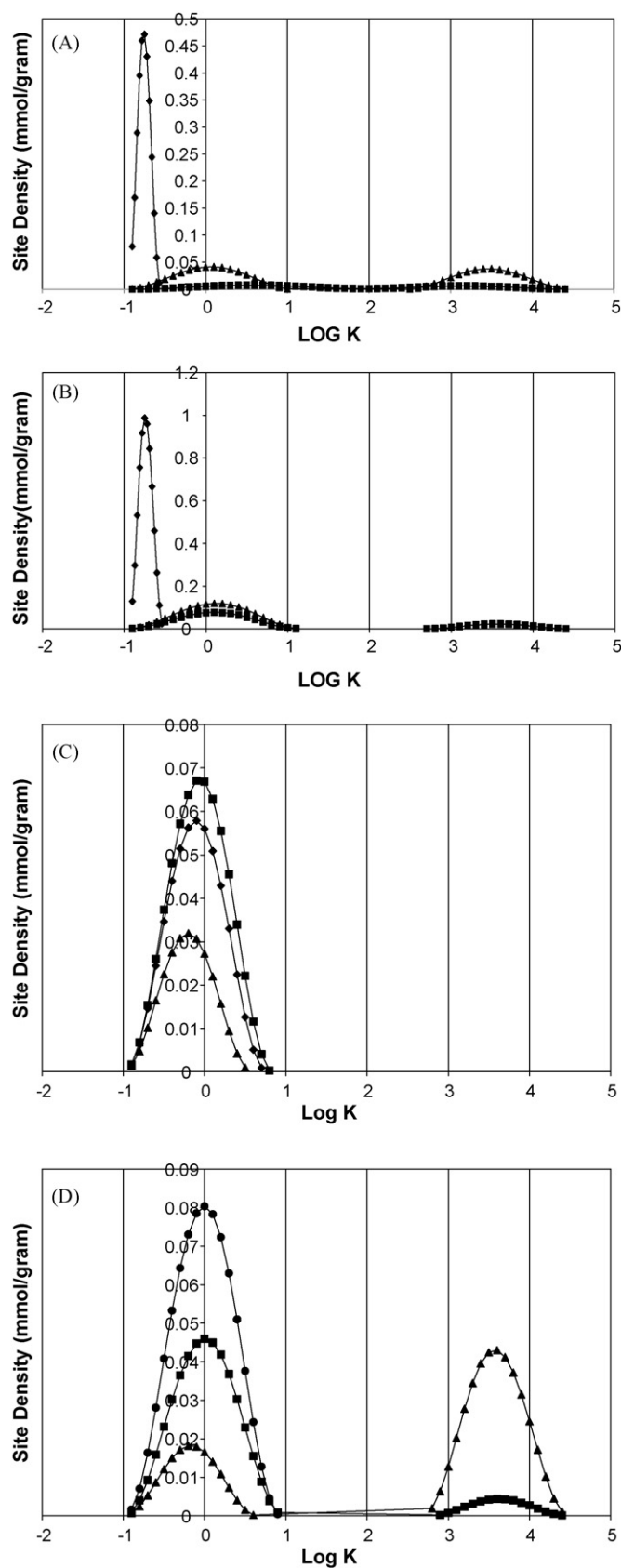


Fig. 5. Affinity spectra derived from binding isotherms generated from deconvolved excitation peak areas under solution conditions of pH 2 (♦), pH 4 (▲), and pH 5 (■) for site 1 (A), site 2 (B), site 3 (C), and site 4 (D).

in the energy of the excited state of the metal ion [17]. It should be noted that binding conditions of pH 5.0 and an initial metal concentration of only 5 mM revealed only a single site corresponding to site 3.

Relating the relative areas of each resulting peak to the total integral of the excitation spectrum, indicative of the total amount of Eu(III) present within each sample, adsorption isotherms could be generated for each site-type. These isotherm data were then subjected to regularized regression analysis using the computer program, QUASI, described above. Figs. 4 and 5 show the resulting affinity spectra for each solution pH (Fig. 4) and each site-type (Fig. 5). At each pH, sites exhibiting a broad distribution (i.e., approximately two orders of magnitude) of low affinity sites. In comparison, the higher pH conditions (i.e., 4 and 5) revealed sites with higher affinities while the more acidic solution indicated the presence of site-types with lower affinities. Variation in apparent affinities of the biosorbed Eu(III) metal ions could be indicative of differences in binding mechanisms ranging from non-specific electrostatic attraction to the cell wall material to ion-exchange processes [17,23], to the formation of surface-metal complexes. This interpretation is consistent with the metal ion binding behavior observed for total metal binding (Fig. 2A). For the purpose of discussion, these mechanisms will be referred to as electrostatic, ion-exchange, and complexation.

Presentation of these same results in Fig. 5 as functions of solution pH for each site-type enables better examination of the impact of solution pH. Electrostatic sites were only observed for sites 1 and 2 at the most acid pH (Fig. 5A and B). This could be explained by the protonation of charged surface sites enabling sub-surface negative charges to dominate metal ion attraction. All four site-types exhibited ion-exchange metal binding of solution pH condition of 4 and 5 and all but site 3 showed a contribution of complexation sites under these same conditions.

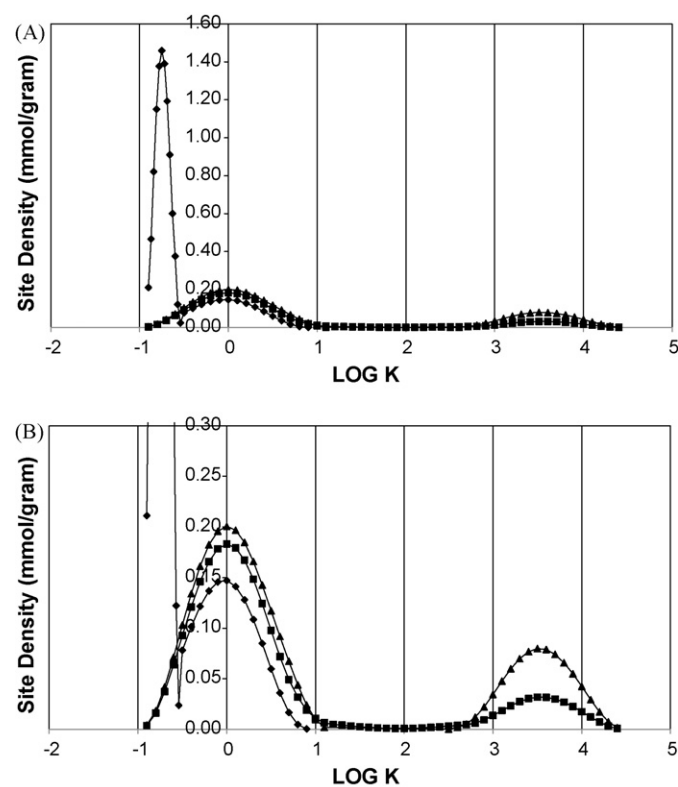


Fig. 6. Total affinity spectra for solution pH conditions of 2 (♦), 4 (▲), and 5 (■) derived from the summation of site-specific results shown in Figs. 4 and 5 (A) with an expanded scale for clarification (B).

If analysis of total metal ion binding isotherm data provides an accurate indication of binding to this chemically heterogeneous material, summation of the site densities for all site-types as a function of the apparent affinities should result in an affinity spectrum similar to that shown in Fig. 2B. Fig. 6 shows such a compilation of site densities. Readily apparent are several notable differences. First is the absence of an indication of the impact of electrostatic sites, although a distribution of sites with lower apparent affinities was observed for pH 2 (Fig. 2B). Second is an apparent shift in binding affinity for both ion-exchange and complexation sites. Finally, analysis of total binding isotherm data revealed apparent affinities three orders of magnitude greater than those observed from site-specific isotherms.

4. Conclusions

Metal ion affinity spectra for Eu(III) binding to chemically distinct sites on a *D. innoxia* cell wall biosorbent have been generated. They have revealed significant differences when such sites are considered and independently compared to a similar analysis of total metal ion binding data. Each of three types of metal-biosorbent interaction has been proposed and includes non-specific electrostatic attractions, ion-exchange processes, and the formation of surface complexes. Efforts to reconstruct total metal binding affinity spectra have indicated the use of such measurements may yield a skewed interpretation of metal binding interactions.

Acknowledgements

The authors gratefully acknowledge the financial assistance of the National Institutes of Health through the MBRS-RISE program (DDS and JLM), and the National Science Foundation Advancement of Graduate Education and the Professoriate (DDS).

References

- [1] B. Volesky, Biosorption and me, *Water Res.* 41 (2007) 4017–4029.
- [2] V.M. Vulava, R. Kretzschmar, U. Rusch, D. Grolimund, J.C. Westall, M. Borovec, Cation competition in a natural subsurface material: modeling of sorption equilibria, *Environ. Sci. Technol.* 34 (2000) 2149–2155.
- [3] T.A. Davis, B. Volesky, A. Mucci, A review of the biochemistry of heavy metal biosorption by brown algae, *Water Res.* 37 (2003) 4311–4330.
- [4] L.R. Drake, G.D. Rayson, Plant materials for metal selective binding and preconcentration, *Anal. Chem.* 68 (1996) 22A–27A.
- [5] A.-C. Texier, Y. Andres, M. Illemassene, D. Le Cloirec, Characterization of lanthanide ions binding sites in cell wall of *Pseudomonas aeruginosa*, *Environ. Sci. Technol.* 34 (2000) 610–615.
- [6] R.H. Crist, K. Oberholser, W. Shank, M. Nguyen, Nature of bonding between metallic-ions and algal cell walls, *Environ. Sci. Technol.* 15 (1981) 1212–1217.
- [7] B. Greene, J.M. Hosea, R. McPherson, M.R.A. Henzl, M.D. Alexander, D.W. Darnall, Interaction of gold(I) and gold(III) complexes with algal biomass, *Environ. Sci. Technol.* 20 (1986) 627–632.
- [8] H.Y. Xia, G.D. Rayson, Solid-state ^{113}Cd NMR studies of metal binding to a *Datura innoxia* biomaterial, *Adv. Environ. Res.* 4 (2000) 69–77.
- [9] H.Y. Xia, G.D. Rayson, ^{113}Cd NMR spectrometry of Cd binding sites on algae and higher plant tissues, *Adv. Environ. Res.* 7 (2002) 157–167.
- [10] J.L. Gardea-Torresdey, K.J. Tiemann, G. Gamez, K. Dokken, Effects of chemical competition for multi-metal binding by *Medicago sativa* (alfalfa), *J. Hazard. Mater.* 69 (1999) 41–51.
- [11] J.L. Gardea-Torresdey, S. Arteaga, K.J. Tiemann, R. Chinaelli, N. Pingatore, W. Mackay, Absorption of copper(II) by creosote bush (*Larrea tridentata*): use of atomic and X-ray absorption spectroscopy, *Environ. Toxicol. Chem.* 20 (2001) 2572–2579.
- [12] S. Lin, L.R. Drake, G.D. Rayson, Applications of frontal affinity chromatography to the study of interactions between metal ions and a complex biomaterial, *Anal. Chem.* 68 (1996) 4087–4093.
- [13] K.H. Chong, B. Volesky, Description of 2-metal biosorption by Langmuir-type models, *Biotechnol. Bioeng.* 47 (1996) 451–460.
- [14] S. Schiewer, B. Volesky, Modeling of the proton-metal ion exchange in biosorption, *Environ. Sci. Technol.* 29 (1995) 3049–3058.
- [15] S. Schiewer, B. Volesky, Modeling multi-metal ion exchange in biosorption, *Environ. Sci. Technol.* 30 (1996) 2921–2927.
- [16] M. Cernik, M. Borkovec, J.C. Westall, Regularized least-squares methods for the calculation of discrete and continuous affinity distributions for heterogeneous sorbents, *Environ. Sci. Technol.* 29 (1995) 413–425.
- [17] S. Lin, L.R. Drake, G.D. Rayson, Affinity distributions of lead ion binding to an immobilized biomaterial derived from cultured cells of *Datura innoxia*, *Adv. Environ. Res.* 6 (2002) 523–532.
- [18] L.R. Drake, C.E. Hensman, S. Lin, G.D. Rayson, P.J. Jackson, Characterization of metal ion binding sites on *Datura innoxia* using Lanthanide ion probe spectroscopy, *Appl. Spectrosc.* 51 (1997) 1476–1483.
- [19] H.Y. Ke, E.R. Birnbaum, D.W. Darnall, G.D. Rayson, P.J. Jackson, Investigation of Eu(III) binding sites on *Datura innoxia* using Eu(III) luminescence, *Appl. Spectrosc.* 46 (1992) 479–488.
- [20] P.A. Williams, G.D. Rayson, Simultaneous multi-element detection of metal ions bound to a *Datura innoxia* material, *J. Hazard. Mater.* 99 (2003) 277–285.
- [21] N.E. Good, G.D. Winget, W. Winter, T.N. Connolly, S. Izawa, R.M.M. Singh, Hydrogen ion buffers for biological research, *Biochemistry* 5 (1966) 467.
- [22] L.R. Drake, T.R. Baker, P.C. Stark, G.D. Rayson, A laser based spectrofluorometer for the efficient probing of metal ion binding sites on solid biomaterials, *Instrum. Sci. Technol.* 23 (1995) 57–69.
- [23] J.L. Gracés, F. Mas, J. Puy, Affinity distribution junctions in multicomponent heterogeneous adsorption. Analytical inversion of isotherms to obtain affinity spectra, *J. Chem. Phys.* 120 (2004) 9266–9276.